

DETERMINATION OF THE SORET COEFFICIENT IN
A THERMODIFFUSION COLUMN BY THE
TRANSIENT METHOD. II

G. D. Rabinovich and M. A. Bukhtilova

UDC 621.039.341.6

The Soret coefficient was measured by the transient method in a thermodiffusion column, for binary mixtures with a low concentration of one component, following a theoretical review of this method as to its applicability to this special case.

It has been shown in [1] that, in the case of a binary mixture being partitioned in a thermodiffusion column closed at both ends, it is necessary to omit the stipulation of zero fluxes at the column ends from the mathematical formulation of the boundary conditions for the transient process, inasmuch as in such a column there always appear end regions where the stream reverses direction.

This method of determining the Soret coefficient on the basis of such a physical model will be proved valid here for the case where the concentration of one component is low, i. e., where the nonlinear term $c(1-c)$ in the transport equation may be replaced by the concentration c .

We note that the low-concentration range is of practical interest, inasmuch as one can establish here the feasibility of using thermodiffusion as a technological process for high-grade purification of substances.

In this case, then, the problem reduces to that of solving the differential equation

$$\frac{\partial c}{\partial \theta} = \frac{\partial^2 c}{\partial y^2} - \frac{\partial c}{\partial y} \quad (1)$$

with the boundary conditions

$$y_e \omega_i \frac{\partial c}{\partial \theta} \Big|_{y=0} = \left(\frac{\partial c}{\partial y} - c \right)_{y=0}, \quad (2)$$

$$y_e \omega_e \frac{\partial c}{\partial \theta} \Big|_{y=y_e} = \left(c - \frac{\partial c}{\partial y} \right)_{y=y_e} \quad (3)$$

and the initial condition

$$c|_{\theta=0} = c_0. \quad (4)$$

The solution to (1) with constraints (2)-(4) is, in Laplace-Carson transforms,

$$\begin{aligned} \bar{c} - c_0 = & \frac{c_0}{p} e^{\frac{y}{2}} \left\{ e^{-\frac{y_e}{2}} \left[\lambda \operatorname{ch} \lambda y + \left(\frac{1}{2} + y_e \omega_i p \right) \operatorname{sh} \lambda y \right. \right. \\ & \left. \left. + \left(\frac{1}{2} - y_e \omega_e p \right) \operatorname{sh} \lambda (y_e - y) - \lambda \operatorname{ch} \lambda (y_e - y) \right] \left\{ \left[1 \right. \right. \right. \\ & \left. \left. \left. + \frac{1}{2} y_e (\omega_e - \omega_i) + y_e^2 \omega_i \omega_e p \right] \operatorname{sh} \lambda y_e + \lambda y_e (\omega_e + \omega_i) \operatorname{ch} \lambda y_e \right\}^{-1} \right\}, \quad (5) \end{aligned}$$

where

$$\lambda = \sqrt{p + \frac{1}{4}}.$$

Institute of Heat and Mass Transfer, Academy of Sciences of the BSSR, Minsk. Translated from *Inzhenerno-Fizicheskii Zhurnal*, Vol. 26, No. 4, pp. 643-650, April, 1974. Original article submitted June 26, 1973.

© 1975 Plenum Publishing Corporation, 227 West 17th Street, New York, N.Y. 10011. No part of this publication may be reproduced, stored in a retrieval system, or transmitted, in any form or by any means, electronic, mechanical, photocopying, microfilming, recording or otherwise, without written permission of the publisher. A copy of this article is available from the publisher for \$15.00.

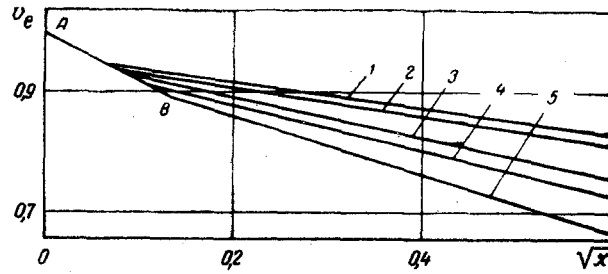


Fig. 1. Linear approximation of Eq. (8): 1) $y_e \omega_e = 8$; 2) $y_e \omega_e = 6$; 3) $y_e \omega_e = 3.33$; 4) $y_e \omega_e = 2$; 5) $y_e \omega_e = 0.25$.

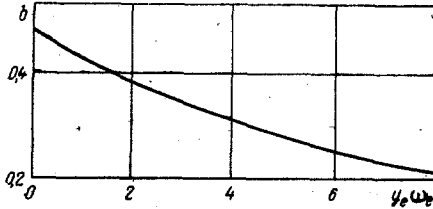


Fig. 2. Slope b as a function of the parameter $y_e \omega_e$ in formula (10).

For the positive end of the column ($y = y_e$) we have

$$\bar{c}_e - c_0 = \frac{c_0}{p} \cdot \frac{\lambda \operatorname{ch} \lambda y_e + \left(\frac{1}{2} + y_e \omega_i p \right) \operatorname{sh} \lambda y_e - \lambda \exp(y_e/2)}{\left[1 + \frac{1}{2} y_e (\omega_e - \omega_i) + y_e^2 \omega_i \omega_e p \right] \operatorname{sh} \lambda y_e + \lambda y_e (\omega_e + \omega_i) \operatorname{ch} \lambda y_e} \quad (6)$$

Inasmuch as we are interested here in the process kinetics during the initial period, it is permissible to let $\operatorname{cosh} \lambda y_e \approx \operatorname{sh} \lambda y_e$ in Eq. (6) and thus replace it by the following equation

$$\bar{c}_e - c_0 = \frac{c_0}{y_e \omega_e p} \left(1 - \frac{1}{y_e \omega_e} \cdot \frac{1}{\lambda + 1/y_e \omega_e + 1/2} \right) \quad (7)$$

An inverse transformation yields the original function

$$\begin{aligned} v_e = & \frac{1}{2k+1} + \frac{1}{2k+1} \left[1 + \frac{(2k-1)(4k^2+1)}{2(2k+1)x} \right] \operatorname{erf} \frac{\sqrt{x}}{2k-1} \\ & + \frac{2k-1}{2k+1} \frac{1}{\sqrt{\pi x}} \exp \left[-\frac{x}{(2k-1)^2} \right] + \frac{2k(2k-1)}{x(2k+1)^2} \\ & \times \exp \left(\frac{2k+1}{2k-1} x \right) \operatorname{erfc} \left(\frac{2k}{2k-1} \sqrt{x} \right) - \frac{2k(2k-1)}{x(2k+1)^2}, \end{aligned} \quad (8)$$

where

$$v_e = \frac{c_e - c_0}{2c_0} \frac{2k-1}{x}; \quad x = \theta \left(k - \frac{1}{2} \right)^2; \quad k = \frac{1}{y_e \omega_e} + \frac{1}{2} \quad (9)$$

It is evident, according to (8), that for a short time the change in concentration at the positive column end will not be affected by the size of the end region on the negative side.

Equation (8) is amenable to a linear approximation:

$$v_e = a - b_1 \bar{x}, \quad (10)$$

as indicated in Fig. 1. Unlike in the case where $c(1-c) = \text{const}$, which has been considered earlier [1], here parameters a and b in (10) are functions of the parameter $y_e \omega_e$, but this relation is a weak one for a and, with an error not exceeding 1%, $a \approx 0.965$. As to slope b , its relation to $y_e \omega_e$ is shown graphically in Fig. 2.

For very short time periods, when the exponential function and the probability integral may, with sufficient accuracy, be replaced by the first two terms of their respective series expansions, Eq. (8) becomes

$$v_e = 1 - \frac{4}{3} \sqrt{\frac{x}{\pi}} \quad (11)$$

The linear range corresponding to condition (11) is represented in Fig. 2 by segment AB with the slope $b = 4/3\sqrt{\pi}$.

Substituting for v and x their values, and taking into account the expressions for θ , y_e , and ω (see NOTATION), we may rewrite formula (10) as follows:

TABLE 1. Geometrical Parameters of the Thermodiffusion Column

Distance from upper end of the outer cylinder, mm	Mean inside diameter of the outer cylinder, mm	Mean outside diameter of the inner cylinder, mm	Mean diameter of centering spacers, mm	
			upper	lower
8	49,970 ± 0,0025		49,925 ± 0,0020	
100	49,972 ± 0,0025	49,421 ± 0,0020		
150	49,968 ± 0,0025	49,422 ± 0,0020		
250	49,975 ± 0,0025	49,426 ± 0,0020		
300	49,976 ± 0,0025	49,421 ± 0,0020		
387	49,976 ± 0,0025			49,931 ± 0,0020

Note: Mean active gap $\delta = 0.274$ mm, active column length $L = 340$ mm, and volume of upper end region $V = 4.1$ cm³.

$$\frac{(\Delta c)_e}{\tau} = h - n \sqrt{\tau}, \quad (12)$$

where

$$h = ac_0 \frac{H}{M}; \quad n = bc_0 \frac{H}{M^2} \sqrt{mK}. \quad (13)$$

Expressions (13) differ from those given in [1] by containing c_0 instead of $\psi = c(1-c)$.

With h and n are determined experimentally, we will thus have

$$\frac{h^2}{n} = c_0 \frac{a^2}{b} \cdot \frac{H}{\sqrt{mK}}; \quad \frac{h}{n} = \frac{a}{b} \cdot \frac{M}{\sqrt{mK}} = \omega L \frac{a}{b} \sqrt{\frac{m}{K}}, \quad (14)$$

from where

$$s \sqrt{D} = \sqrt{\frac{10}{7}} \cdot \frac{bh^2}{c_0 a^2 n} \cdot \frac{\delta}{\Delta T}; \quad \omega_e \sqrt{D} = \frac{1}{\sqrt{9!}} \frac{bh}{an} \frac{g\rho\beta\delta^3\Delta T}{\eta L}. \quad (15)$$

When using formulas (15), one must remember that slope b is a function of $y_e\omega_e$, as has been noted earlier. With ω_e replaced according to (15) and y_e replaced by its value according to the adopted notation, this parameter $y_e\omega_e$ becomes

$$y_e\omega_e = \sqrt{\frac{7}{10}} \cdot \frac{bh}{an} \cdot \frac{\Delta T}{\delta} \cdot s \sqrt{D},$$

or, according to the first equation in (15),

$$y_e\omega_e = \frac{h^3 b^2}{c_0 a^3 n^2}. \quad (16)$$

The last expression establishes, for any specific experiment, a unique relation between $y_e\omega_e$ and the slope, namely

$$b = nc_0^{1/2} \left(\frac{a}{h}\right)^{3/2} \sqrt{y_e\omega_e}. \quad (17)$$

When relation (17) is represented by a graph, then its intersection with the curve in Fig. 2 will yield the sought value of b to be used for calculations according to formulas (15).

With θ , y_e , and ω replaced by their values, we have for x :

$$x = mK\tau/M^2,$$

whence, in view of the second equation in (14),

$$\tau = \left(\frac{bh}{an}\right)^2 x. \quad (18)$$

We will now determine for how long periods of time τ formula (11) is still applicable. According to Fig. 1, at the positive column end the validity range of formula (11) narrows down as the value of parameter $y_e\omega_e$ increases, and is $0.006 < x < 0.025$ at the values of $y_e\omega_e$ specified on the diagram.

Taking the average of the given values ($x = 0.015$), for example, then, with $y_e\omega_e = 2$ for mixture No. 1 (see Table 2), we find that formula (11) is applicable only during less than 4 min.

TABLE 2. Data on Binary Mixtures and Operating Temperatures in the Thermodiffusion Column for Measurements of the Soret Coefficient

No.	Test mixture		C ₀ (molar fraction)		D · 10 ⁹ , m ² /sec	β · 10 ³ , deg ⁻¹	η · 10 ³ , N · sec /m ²	ρ · 10 ³ , kg/m ³	T ₁ , °K	T ₂ , °K	T̄, °K	ΔT, °K
	I	II	I	II								
1	CCl ₄	C ₆ H ₁₄	0,9612	0,0388	1,487 [2]	1,23	0,791	1,556	328	298	308	30
2	CCl ₄	C ₆ H ₁₂	0,9648	0,0352	1,34 [3]	1,23	0,791	1,556	328	298	308	30
3	CCl ₄	C ₆ H ₆	0,9578	0,0422	1,79 [2]	1,23	0,791	1,556	328	298	308	30
4	CCl ₄	C ₆ H ₆	0,9767	0,0233	1,79 [2]	1,23	0,791	1,556	328	298	308	30

Note: Coefficients β and η, as well as the density, are assumed the same as for component I.

It is technically difficult to carry out such an experiment in a column during such a short time, of course, and the tests must be performed within the range on the right-hand side of point B in Fig. 1.

Formulas (15) were used for evaluating the Soret coefficient on the basis of measurements in columns.

The tests were performed in an apparatus consisting essentially of a column made up of two coaxial cylinders. The geometrical parameters of this column are given in Table 1.

Since the inner cylinder comprised the hot surface, hence the gap width was throughout the experiment smaller than nominal (specified in Table 1) by $\alpha d(T_1 - 293)$, with α denoting the linear expansivity of structural steel and d denoting the outside diameter of the inner cylinder. The tests were performed at the temperature $T_1 = 328^\circ\text{K}$, corresponding to $\delta = 0.266$ mm. The allowance for expansion of the centering spacers at this temperature did not, however, ensure their contact with the inside surface of the outer cylinder and did not preclude the possibility of a misalignment between the cylinders during the assembly of the column so that their eccentricity, in fact, could fluctuate from 0 to 20 μ , i. e., the average eccentricity was $\epsilon = 10 \mu$ or $\epsilon/\delta = 3.8\%$.

The upper end region of the column remained within the active zone and was contained by seals. The lower end region was eliminated by filling it with a Teflon collar. The inner cylinder was heated with hot water from a model U-10 thermostat. The temperature was measured with twelve copper-constantan thermocouples, six on each thermostaticized surface.

The theoretical justification of determining the Soret coefficient by this method is based on our ability to establish the kinetics of partitioning a binary mixture within a rather short time. For this reason, the reliability of the final results depended very much on developing the experimental technique by which the boundary conditions could be established in accordance with the mathematical formulation of the problem.

This required a steady temperature distribution in the apparatus and a uniform concentration profile along the column height at time zero. These conditions were met in the following way: the thermostats were turned on and some time later the mixture for the partition test was poured from the lower end while being drained into a sampler in the upper end at such a rate that no vertical concentration gradient would appear, i. e., the column was operated in the sampling mode with a concentration c_0 maintained at one of its ends. It can be shown that in this case, when $c \ll 1$, the partition index was

$$\frac{c_e}{c_0} = q = 1 + \frac{1}{\kappa} \quad (19)$$

Considering that the requirement of a nearly zero gradient along the column height was met when $q = 1.005$, we found the factor $\kappa = \sigma/H \geq 500$. For most organic mixtures H is of the order of 10^{-7} – 10^{-5} kg/sec, i. e., the sampling rate must exceed 10^{-5} kg/sec. For this reason, the sampling operation has been designed to last only a few minutes at a rate of approximately 3 g/min. During this time an entire column volume was displaced and a steady temperature was established across the gap, this temperature being measured with thermocouples.

As both the upper and the lower sampler were covered again, we started the stopwatch and began counting time.

The mixture parameters and the operating temperatures are listed in Table 2.

TABLE 3. Results of Test Data Evaluation Pertaining to a Determination of the Soret Coefficient in Binary Mixtures

Test mixture (see Table 2)	$h \cdot 10^5$, sec^{-1}	$n \cdot 10^7$, $\text{sec}^{-3/2}$	ω according to (16)	$S \cdot 10^3, \text{sec}^{-1}$		
				according to (15)	according to (20)	cell tests
1	2,50	2,63	0,0709	7,55	3,18	12,0 [4]
2	1,02	0,803	0,106	5,03	2,07	5,05 [3]
3	1,30	1,04	0,0875	4,46	2,07	5,4 [5]
4	0,94	0,855	0,0775	5,42	2,2	5,8 [6]

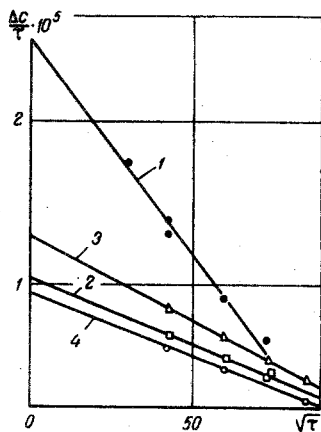


Fig. 3. Ratio $\Delta c/\tau$ (sec^{-1}) as a function of $\sqrt{\tau}$ ($\text{sec}^{1/2}$), for mixtures No. 1, 2, 3, 4 (see Table 2).

angles (with the axis of abscissas) and the intercepts (on the axis of ordinates), along with the values of the Soret coefficient based either on the first formula in (15) or on the Ruppel—Coull formula [11] for the initial segment of the kinetic curve:

$$\Delta c = 2c_0 \sqrt{\frac{\theta}{\pi}}, \quad (20)$$

under conditions of sampling from one end of a column closed at both ends. Formula (20) had been derived by solving Eq. (1) under the condition of zero fluxes at both ends of the column, i. e., under conditions not corresponding to the true physical pattern, as was mentioned at the beginning of this article. Table 3 indicates that the values of s calculated according to formula (20) are more than twice as high as those based on the method we propose here. In the last column of Table 3 are given values obtained for the same mixtures by other authors in cell tests.

Evidently, the values obtained by cell tests are somewhat higher than those obtained here. This discrepancy should be attributed to the geometrical imperfection of our column, namely by the rather large eccentricity between inner and outer cylinder, which has been discussed earlier.

It has been noted in [9] that the values of the Soret coefficient according to test data already available are much lower than those predicted by theory. This and the results in [1] based on the evaluation of data in [10] are evidence in favor of continuing further research in columns of a more nearly perfect geometry, where parasitic convection can be minimized and the final values of the Soret coefficient are more reliable.

Nevertheless, the data shown here indicate already that a carefully assembled thermodiffusion column may serve as an excellent instrument for determinations of the Soret coefficient.

In conclusion, we must say something about the quantity ω representing the ratio of the volume of an end region, where the convective stream reverses in a column, to the total volume of the column. With the physical properties of the partitioned mixture known, this quantity has been calculated here according to formulas (15) and its values are listed in Table 3. It is noteworthy that this quantity fluctuates within

narrow limits for three out of four test mixtures, suggesting that it characterizes the column design rather than the mixture composition. This hypothesis requires further testing for confirmation and, if proved correct, will render formulas (15) suitable for determining both the Soret coefficient and the diffusivity at the same time.

NOTATION

c	is the concentration;
$0 = H^2\tau/mK$;	
$H = sg\rho^2\beta\delta^3(\Delta T)^2B/6\eta$;	
$K = g^2\rho^3\beta^2\delta^7(\Delta T)^2B/9\eta^2D$;	
$m = \rho B\delta$;	
τ	is the time;
ρ	is the density;
β	is the volume expansivity;
δ	is the gap width;
$\Delta T = T_1 - T_2$;	
$\bar{T} = 1/2(T_1 + T_2)$;	
T_1	is the temperature of the hot surface;
T_2	is the temperature of the cold surface;
B	is the gap perimeter;
η	is the dynamic viscosity;
D	is the diffusivity;
$y = Hz/K$;	
z	is the vertical coordinate;
$y_e = HL/K$;	
L	is the active column height;
$\omega = M/mL$;	
M	is the mass of the mixture to be partitioned and filling the volume of the end regions;
ϵ	is the eccentricity;
s	is the Soret coefficient.

Subscripts

e	refers to the positive end of a column;
i	refers to the negative end of a column;
0	refers to the initial condition.

LITERATURE CITED

1. G. D. Rabinovich, *Inzh. Fiz. Zh.*, **26**, No. 3 (1974).
2. Landolt-Börnstein, Part 5, Vol. A, Springer Verlag, Berlin (1969).
3. C. Anderson and H. Horne, *J. Chem. Phys.*, **55**, 2831 (1971).
4. G. I. Bobrova and M. A. Bukhtilova, *Inzh. Fiz. Zh.*, **22**, 339 (1972).
5. J. Turner, B. Butler, and M. Story, *Trans. Faraday Soc.*, **63**, 1906 (1967).
6. M. Story and J. Turner, *Trans. Faraday Soc.*, **65**, 349 (1969).
7. J. Demicjowicz-Pigoniowa, M. Mitchell, and H. Tyrrell, *J. Chem. Soc. (A)*, 307 (1971).
8. J. Shieh, *J. Phys. Chem.*, **75**, 1508 (1969).
9. L. S. Kotousov, *Doctoral Dissert.*, Leningrad (1970).
10. T. R. Bott and J. J. B. Romero, *Trans. Inst. Chem. Engrs.*, **47** T, 166 (1969).
11. T. C. Ruppel and J. Coull, *Industr. Chem. Engrg. Fundamentals*, **3**, 162 (1964).